A Coordinated Control of Offshore Wind Power and BESS to Provide Power System Flexibility

Martha N. Acosta [1], Francisco Gonzalez-Longatt [1,*], Juan Manuel Roldan-Fernandez [2] and Manuel Burgos-Payan [2,*]

[1] Department of Electrical Engineering, Information Technology and Cybernetics, University of South-Eastern Norway, 3918 Porsgrunn, Norway; Martha.Acosta@usn.no

[2] Department of Electrical Engineering, Universidad de Sevilla, 41004 Seville, Spain; jmroldan@us.es

* Correspondence: fglongatt@fglongatt.org (F.G.-L.); mburgos@us.es (M.B.-P.)

Abstract: The massive integration of variable renewable energy (VRE) in modern power systems is imposing several challenges; one of them is the increased need for balancing services. Coping with the high variability of the future generation mix with incredible high shares of VER, the power system requires developing and enabling sources of flexibility. This paper proposes and demonstrates a single layer control system for coordinating the steady-state operation of battery energy storage system (BESS) and wind power plants via multi-terminal high voltage direct current (HVDC). The proposed coordinated controller is a single layer controller on the top of the power converter-based technologies. Specifically, the coordinated controller uses the capabilities of the distributed battery energy storage systems (BESS) to store electricity when a logic function is fulfilled. The proposed approach has been implemented considering a control logic based on the power flow in the DC undersea cables and coordinated to charging distributed-BESS assets. The implemented coordinated controller has been tested using numerical simulations in a modified version of the classical IEEE 14-bus test system, including tree-HVDC converter stations. A 24-h (1-min resolution) quasi-dynamic simulation was used to demonstrate the suitability of the proposed coordinated control. The controller demonstrated the capacity of fulfilling the defined control logic. Finally, the instantaneous flexibility power was calculated, demonstrating the suitability of the proposed coordinated controller to provide flexibility and decreased requirements for balancing power.

Keywords: battery energy storage; charging/discharging control; coordinated control; flexibility; offshore wind power

1. Introduction

The International Renewable Energy Agency (IRENA) [1] suggested that by 2050, globally, around 61% of electricity could be supplied by variable renewable energy (VRE) sources like solar and wind power (WP). Consequently, the electrical power system is quickly migrating the generation mix toward more environmentally friendly generation technologies. Simultaneously, the requirement for balancing the energy supply and demand becomes more and more complex as a result of VRE integration. Coping with the high variability of the future generation mix with incredible high shares of VER, the power system requires developing and enabling sources of flexibility. The reliable operation of the power systems with a high penetration of VRE requires a well-planned and fully used flexibility at all levels of the power system. It includes enabling the maximum flexibility from the power generation to the transmission/distribution system, but also enabling the demand side flexibility; in this process, energy storage plays a very important role.

Power system flexibility is related to the ability of the power system to manage changes. It is, generally speaking, a property of the power system that describes its ability to cope with events that may cause imbalances between supply and demand in different

time frames. Flexibility management is one very important mechanism to preserve system reliability at a cost.

The CIGRE working group C5.27, Market Design for Short-Term Flexibility, defines flexibility as "a characteristic of capacity. If we view capacity as the possibility (or option) to either consume or produce electrical energy, then flexibility is the capability to use this capacity freely and to adapt the capacity responding to price signals" [2]. In the UK, the term flexibility refers to the ability to react to the fluctuating needs of the power system, maintaining the security of supply [3].

Some of the quantifiable dimensions of flexibility are as follows:

- Flexibility power: Refers to the physical capability to deliver flexible power, e.g., the size of the flexible active or reactive load, expressed in MW for active power flexibility or presented on MVAr for reactive power flexibility.
- Flexibility response time: It is defined as the time until the flexibility (for instance, flexible power) can be delivered, e.g., related to the start-up time of a power plant, expressed in seconds–minutes–hours–days–years. Power electronic-based technologies are very effective in terms of the very short flexibility time response enabled on them. However, it is important to consider the speed response of the primary energy source, e.g., extremely short for ultra-capacitors and relatively small for some types of battery energy storage systems.
- Flexibility speed: The rate at which the flexibility can be delivered. It is typically defined as a rate of change where the flexibility is expressed in terms of the changes over time. For instance, the emergency ramp rate of an HVDC, which is expressed in terms of the active power change over time (MW/s).
- Flexibility duration: Defines how long flexibility can be provided. It is expressed in terms of time, e.g., the time span for the overload rating of a component, expressed in seconds–minutes–hours, etc.
- Flexibility energy: It is the total energy provided by the flexibility; it can be obtained considering the flexibility power and flexibility duration dimensions. As an energy, the typical unit used to represent it is MWh.
- Flexibility recovery period: It is defined as the time interval that is needed in order to provide flexibility after it has been fully utilised, e.g., the time required to reach full state-of-charge (SoC) charge in an empty energy storage system (ESS) after providing it flexibility; it is expressed in units of time, varies from seconds, minutes, hours, or more, depending on the technology used to provide the flexibility.

More details about more flexibility metrics can be found in [2].

Power system flexibility studies have been taking more relevance in recent years because of the high integration of VER. As a result, several methodologies in the scientific literature have studied for the implication of integrating flexible sources to enhance power balancing and cope with the high penetration of VER. For instance, numerous research publications have focussed on creating models for power system flexibility assessment proposes. These models are based on mathematical approaches defining the power system operation limits [4,5], based on indexes [6–8], such as the operational flexibility index, and on charts and graphic tools [9,10]. Furthermore, several methodologies have been proposed to study the variability of the VER using optimisation approaches [11–13] or using the analytical model of the power reserves [14,15]. The variability of the load that VERs cannot cover has been addressed using a recently created service named the flexible ramp product [16–18]. Moreover, different methodologies have been proposed to study the flexibility requisites considering several aspects, such as medium- and long-term planning, dispatch, and unit commitment [19–21]. Lately, numerous studies have been carried out considering the electrical market design in order to assess how it influences power system flexibility [22–26]. A detailed review of the methodologies applied to assess the power system flexibility is presented in [27].

In this paper, the flexibility is fully enabled considering the increased use of digitalisation, which helps to maintain balance on the system efficiently. It considers the extensive

implementation of information and communication technologies and solutions as enablers of the power system flexibility. In addition, this scientific paper considers integration as a key element enabling flexibility.

This paper proposes and demonstrates a single layer control system for coordinating the operation of battery energy storage system (BESS) and wind power plants via multi-terminal high voltage direct current (HVDC). The proposed single-layer coordinating controller is a closed-loop controller that uses wide-area measurements in the system to coordinate several transmission/distribution and energy storage assets. The proposed coordinated controller is a single layer controller on top of the power converter-based technologies. Specifically, the coordinated controller uses the capabilities of the distributed-BESS assets to store electricity when the logic function of the proposed controller is satistied. Section 2 proposed a single layer coordinated controller; it is intended to coordinate the active power injection/abortion of distributed-BESS installed in an AC interconnected multi-machine power system. One very important element of the controller is reaching the coordinated charging/discharging of the BESSs according to the interactions in the multi-terminal DC system where offshore wind power plants inject a variable volume of active power. Section 3 is dedicated to implementing the proposed coordinated controller and discussing the numerical simulation results using a customised version of the IEEE 14-bus, including novel power electronic converter technologies. Finally, the main conclusions and findings are summarised in Section 4.

2. Coordinated Distributed-BESS and Wind Power Plant

Reaching an acceptable reliability level of operation in a power system with a massive penetration of VRE requires taking advantage of all of the possible flexibilities available in the system. Power electronic converters provide an interface with a very fast response; as a consequence, when combined with appropriate energy technology, the result will be a very useful level of flexibility. In this paper, a coordinated BESS and wind power plant is proposed. The proposed controller is intended to coordinate the active power injection/abortion of the distributed-BESS installed in an AC interconnected, multi-machine power system. The key element is coordinating the charging/discharging behaviour of the BESS according to the interactions in the multi-terminal DC system, where the offshore wind power plant injects a variable volume of active power. The general scheme of the main components of the coordinated BESS and wind power plants control is presented in Figure 1.

The proposed coordinated controller is a single layer controller on the top of the power converter-based technologies. Specifically, the coordinated controller uses the capabilities of the distributed-BESS assets to store electricity when the logic function of the proposed controller is satisfied. For instance, the logic function can be implemented in order to allow for the charge of the BESS where the offshore wind power production is such that it surpasses a specific threshold, and then the BESS is used to compensate for the active power reduction of the offshore wind power plants when there are low wind speeds. However, many other logic functions can easily be implemented (as illustrated in the next section). The charge and discharge of the BESS asset are managed considering two control actions. The coordinated controller takes actions at the modular multilevel converter-HVDC (MMC-HVDC) stations located in the AC/DC interface; it is implemented by taking advantage of the local controllers at each one of the MMC-HVDC stations and the voltage−power ($U_{dc}−P_{dc}$) control (see Figure 2).
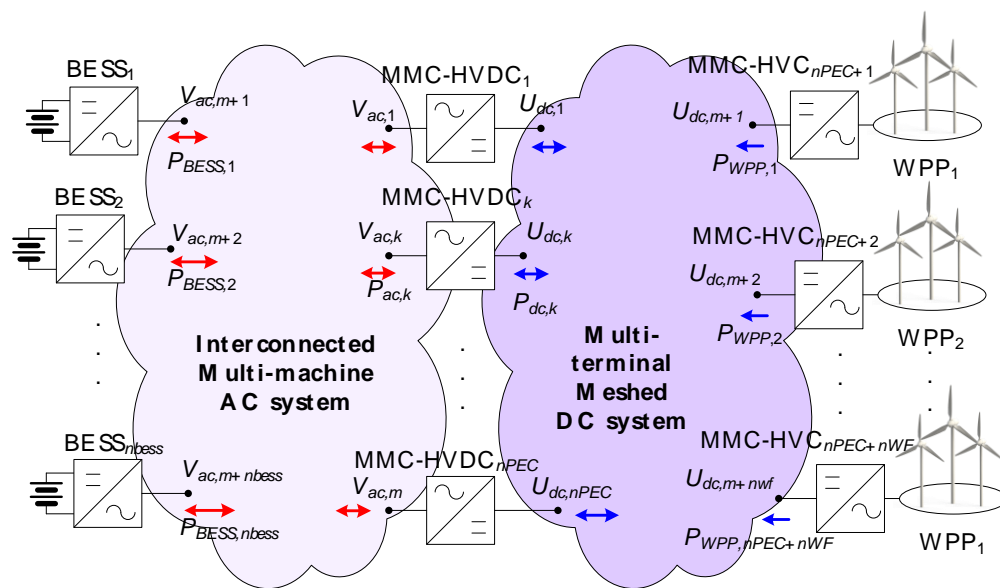
Figure 1. General scheme of the distributed-BESS and wind power plant considering and AC interconnected multimachine system connected to a multi-terminal HVDC system.
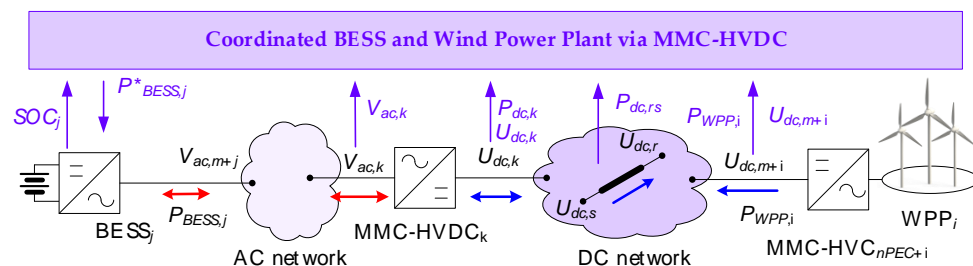

Figure 2. General scheme of the proposed coordinated distributed-BESS and wind power plant controller via a multi-terminal HVDC system.

The charger controller is a local controller that belongs to each one of the distributed BESSs, and it is intended to keep the SoC inside the operational limits ($SoC_{min,j} \leq SoC_j \leq SoC_{max,j}$, $j = 1, \ldots$, *nbess*). The coordinated controller uses digital communication to monitor the SoC of all BESS assets during the time it produces active power references to control the active power injection/consumption. It is based on a coordinated logic between the offshore wind power plants and the multi-terminal DC system, using the MMC-HVDC stations to deliver the required power flow.

A distributed-BESS (BESS$_j$) will charge and discharge based on the reference signal provided by the coordinated controller ($P^*_{BESS,j}$); the local SoC controller will then check if the asset is able to deliver the requested reference based on the actual SoC, delivering the requested reference, if the asset is not able to fulfil the requested reference; and then the coordinated controller will use the next available distributed-BESS based on a priority table created based on the SoC.

The core of the proposed coordinated controller is a logic function that defines the charging and discharging action of the distributed-BESS assets. Many logic functions can be implemented depending on the agreements between the different system operators. For instance, the logic function can be implemented to cope with offshore wind power production variability.

When the total offshore wind power production ($P_{WPPT} = PWPP_1 + \ldots + P_{WWPnwf} < P_{Tref}$) is below the threshold, the coordinated controller will provide reference signals to the charged BESS ($SoC_j > SoC_{min,j}$), the order of discharge starts from the asset with

the larger *SoC* continuing to the less charged BESS. In the opposite situation, the BESS is charged when $P_{WPPT} > P_{Tref}$.

The proposed controller is able to implement any control logic related to AC or DC measurements and AC, DC, or even AC/DC objectives; the only limit is that imposed by the electrical circuit and the power electronic converters. The real implementation of the proposed coordinated controller is very simple. The digitalisation of the power system allows for the integration of digital technologies that offer a very low latency. The time scale of the action taken is in several seconds up to a minute. As a consequence, the modern digital communication technologies (5G wireless and optic fibre) offer almost no time delay on transmitting the measurements or sending back the control commands.

The appropriate infrastructure for the control is already available in many commercially available power converters. The very well know IEC 61850 standard enables substation automation by standardising communication between devices from different manufacturers. The implementation of the IEC 61850 GOOSE (Generic Object-Oriented Substation Event) and the Manufacturing Message Specification (MMS) allows for a simple way to implement control actions in power electronic converters and so many other technologies. There are very well documented experiences regarding the use of IEC TR 61850-90-7 and UL 1741 standards in the development of the control of the so-called smart PV inverters [28].

2.1. Voltage Control in DC Transmission Systems

Several topologies are available regarding the implementation of PWM (pulse-width modulation) power converter stations for DC transmission system applications: self-commutated, voltage-source AC/DC two-level converter, and a modular multilevel converter (MMC). The use of MMCs is the power electronic converter (PEC) topology of choice for a voltage source converter (VSC) high voltage direct current DC (VSC-HVDC) transmission system. Several technical and economic reasons make them very attractive for VSC-HVDC [29], including the very high efficiency (reducing losses through voltage levels to build an output waveform) and technical features, such as a very fine and compact power control and back start functionalities.

The modelling of power converter stations based on MMC-HVDC systems requires special attention to the details. In this paper, the implemented MMC-HVDC station is based on a full-bridge configuration (also called H-bridge), as presented in Figures 3 and 4 [30].
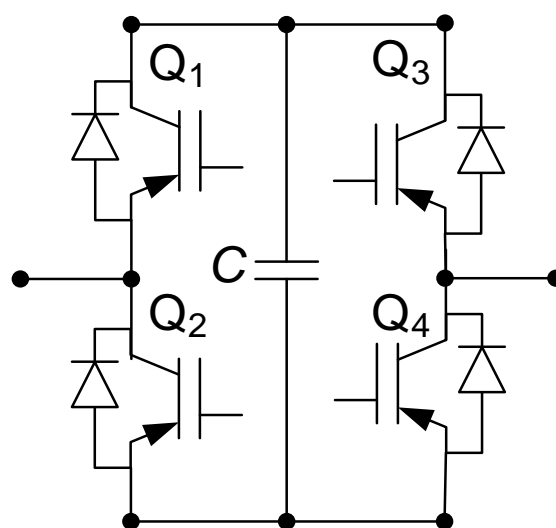

Figure 3. Representative electrical circuit diagram of a full-bridge submodule used in an MMC-HVDC converter station.
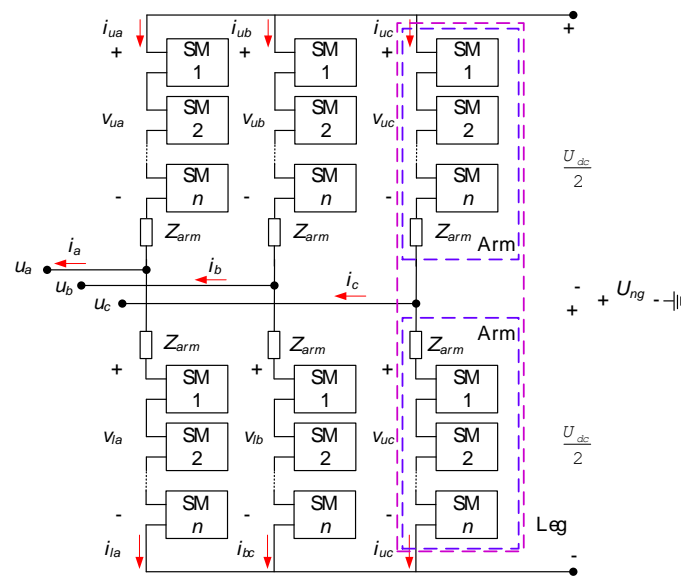
Figure 4. Representative electrical circuit diagram of an MMC-HVDC station: Arm and leg are highlighted in the circuit.

Steady-state conditions of the MMC-HVDC station are controlled using the modulation index. The line−line AC voltage at the node k (rms value, $V_{ac,k} = V_{ac,k,d} + jV_{ac,k,q}$) and DC voltage ($U_{dc,k}$) are related by the following:

$$V_{ac,k,d} = \frac{\sqrt{3}}{2\sqrt{2}} m_{d,k} U_{dk,k} \tag{1}$$

$$V_{ac,k,q} = \frac{\sqrt{3}}{2\sqrt{2}} m_{q,k} U_{dk,k} \tag{2}$$

where $m_{d,k}$ and $m_{q,k}$ are the real and imaginary part of the modulation index (m_k), respectively.

Several control modes are possible at the MMC-HVDC station; for simplicity in this scientific paper, three main control technologies are presented and used for illustrative purposes in the next section.

2.1.1. Control Mode U_{dc}-Q_{ac}

This control mode allows for controlling the voltage on the DC side (U_{dc}) of the MMC-HVDC station, and the time to control the reactive power (Q_{ac}) is on the AC side. This control method is used for many applications, including FACTS like STATACOM, shunt-converter in the UPFC configuration, type 3 wind turbine generators (grid-side converter of the doubly-fed induction generator), and MMC-VDC-HVDC systems. More information about this control model can be found in [31,32].

2.1.2. Control Mode P_{ac}-Q_{ac}

This control mode is specifically used when the control quantities at the MMC-HVDC stations are the active (P_{ac}) and (Q_{ac}) reactive power at the AC side. This controller is able to replicate the operational PQ mode used to represent a synchronous generator in steady-state conditions. More information about this control model can be found in [33,34].

2.1.3. Control Mode U_{dc}-P_{dc}-*Droop*

It is possible to set the MMC stations using a U_{dc}-P_{dc} characteristic. The typical control rule is the use of a proportional control between the voltage and power. The

DC-voltage dependent P-droop allows for defining the active power setpoint that follows the following equation:

$$P_{dc,ref} = P_{dc,set} + \frac{1}{\rho_{dc}} \{U_{dc} - U_{dc,set}\} \tag{3}$$

where $P_{dc,ref}$ is the reference of $P_{dc,ref}$ used at the MMC-HVDC station, $P_{dc,set}$ is the active power setpoint, U_{dc} is the actual voltage at the DC side of the MMC-HVDC station, $U_{dc,set}$ is the DC voltage setpoint, and ρ_{dc} is the proportionality factor defining the DC-voltage dependent P_{dc}-droop.

2.2. Distributed Battery Energy Storage Systems

The distributed-BESS consists of three components (see Figure 5): (i) an energy storage package, a set of batteries with an appropriate connection to provide; (ii) a power electronic converter model (inverter/rectifier); and (iii) several control loops installed to allow for the proper operation of the energy storage system [35,36].
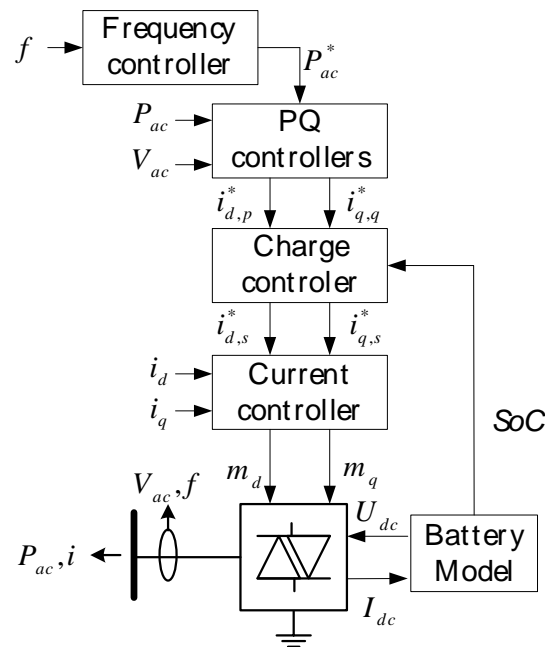

Figure 5. Representative block diagram illustrating the distributed-BESS asset.

An MMC-VSC is used as the interface between the energy storage pack and the AC grid. As this scientific paper is focused on the steady-state of the power system, the performance of the PWM-converter is modelled using an equivalent to the fundamental frequency. The line−line AC voltage (RMS value $V_{ac} = V_{ac,d} + jV_{ac,q}$) and DC voltage ($U_{dc}$) are related by the following:

$$V_{ac,d} = \frac{\sqrt{3}}{2\sqrt{2}} m_d U_{dk} \tag{4}$$

$$V_{ac,q} = \frac{\sqrt{3}}{2\sqrt{2}} m_q U_{dk} \tag{5}$$

where m_d and m_q are the real and imaginary part of the modulation index, respectively.

3. Implementation and Results

In this section, the well-known IEEE 14 bus test system is used to illustrate an implementation of the proposed coordinated control. The IEEE 14 bus test system is a representative example of a reduced area of the American Electric Power System (in the Midwestern

area of the United States of America) as of February 1962. It consists of five synchronous machines, three of which are synchronous compensators (SC) used only for reactive power production and voltage improvement. The IEEE 14 bus system is used to represent the AC interconnected multimachine system (see Figure 6). It has a total of 11 loads for a total load of 259 MW and 81.3 Mvar. The original data of the test system are publicly available at: https://labs.ece.uw.edu/pstca/pf14/pg_tca14bus.htm (accessed on 5 May 2021).
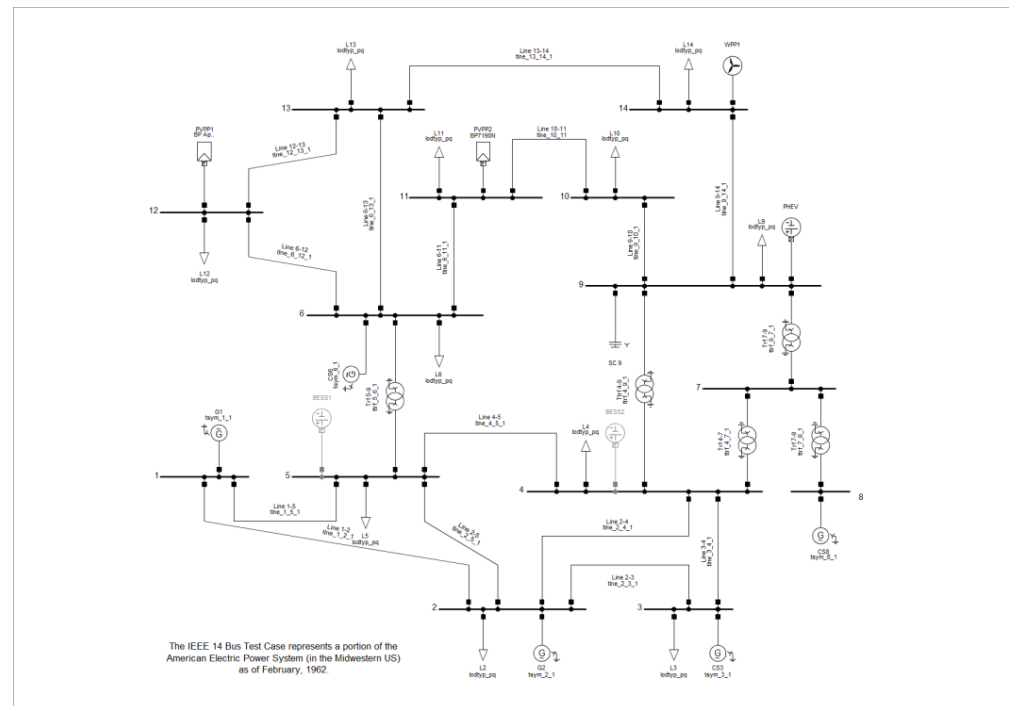
Figure 6. AC test system: A customised version of the IEEE 14 bus test system.

The IEEE 14 bus test system has been customised in this paper in order to integrate new technologies. The following two wind power plants are added: onshore wind farm (WPP1, bus 14, 2 × Gamesa SG10) and offshore wind farm (WPP2, bus 15, 2 × Gamesa SG10). A multi-terminal MMC-HVDC system (three terminals—Figure 7) is used to connect the WPP2 to the IEEE 14 bus system (buses 4 and 5). Two photovoltaic power plants (PVPP1 and PVPP2, bus 11 and 12, respectively), an electric vehicle (PHEV, bus 9), and two distributed-BESSs (bus 4 and 5, 30 MWh each) are added to the network. More details of the customised network can be found in [37].

The proposed coordinated controller is illustrated considering a representative period of 24-h (1-min resolution). Figure 8 shows the load profile of the 11 loads connected in the AC test system, and Figures 9 and 10 show the power production of the PV power plants and wind power plants.
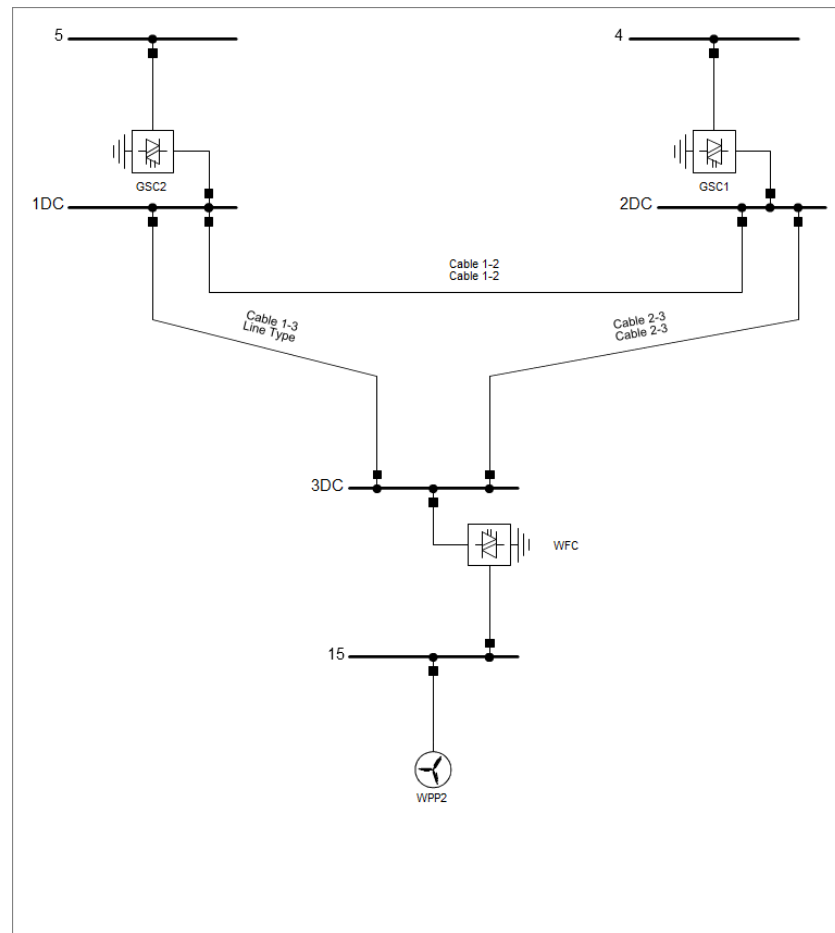
Figure 7. DC test system: three-terminal MMC-HVDC transmission system used to integrate the offshore wind power plant WPP2.
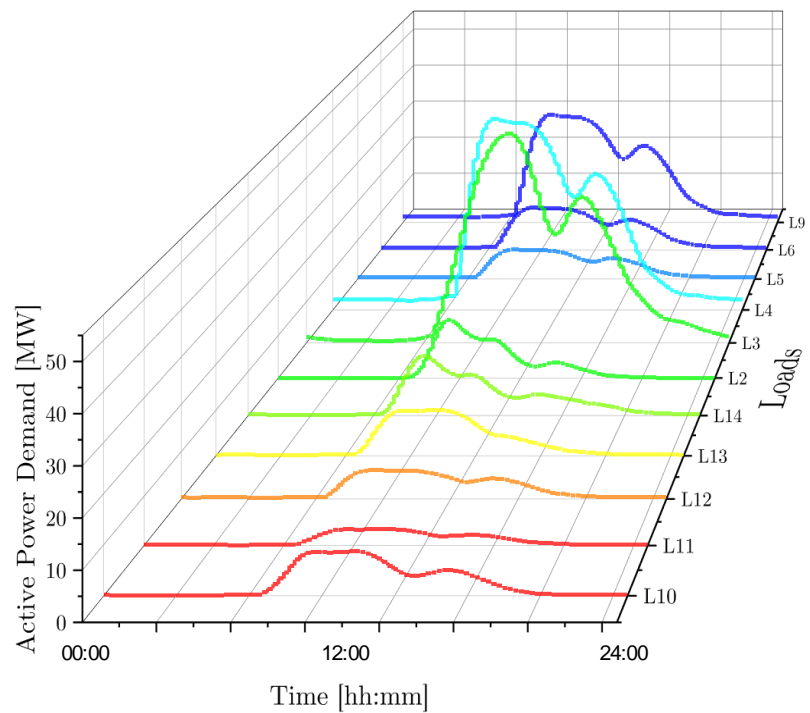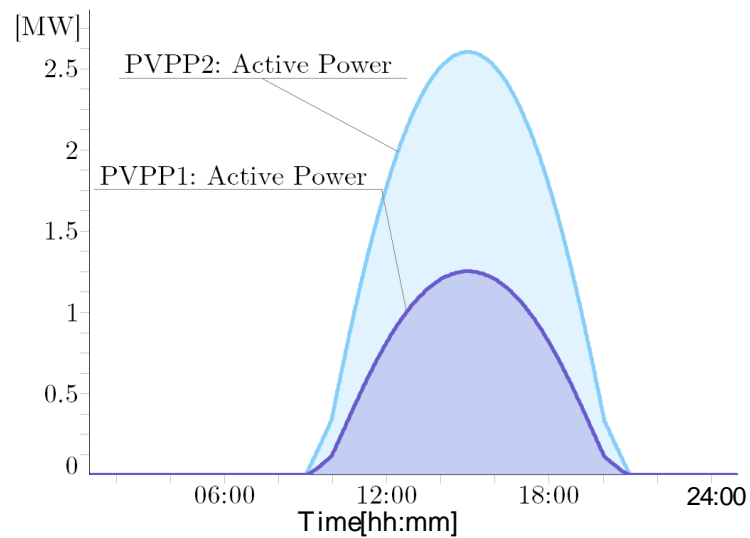

Figure 8. 24-h load profiles of the AC test system.

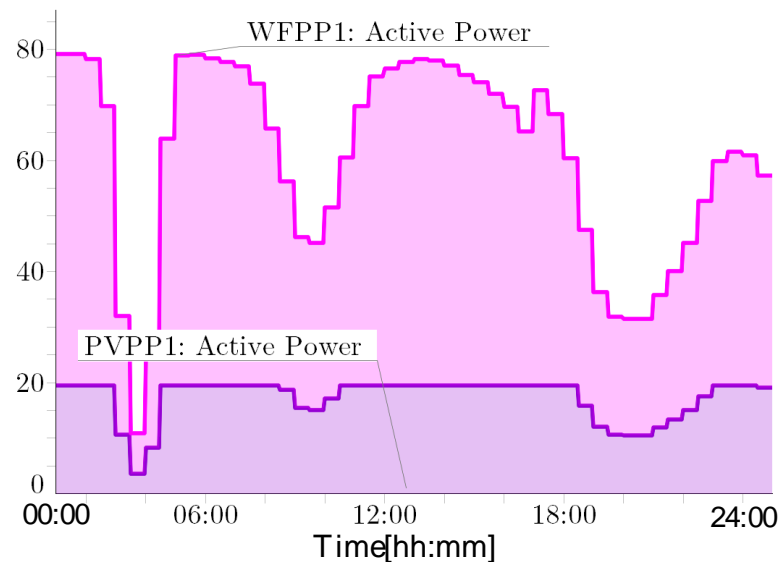**Figure 9.** 24-h generation profiles of the PV power plants.

Figure 10. 24-h generation profiles of the wind power plants: Offshore (WFPP1, 2 × Gamesa SG10) and Onshore (WFPP2, 8 × Gamesa SG10).

In this section, coordinated control has been implemented in a very challenging way. The multi-terminal MMC-HVDC system uses three undersea cables (delta connection) to transport the power production of the offshore wind power plant (P_{WPP2}), as presented in Figure 10. The power production of the offshore wind farm has periods reaching the rated power, but there are also periods where the power production is very reduced (~7MA @2:57am). As the DC-undersea cables are connected to a monopolar MMC-converter configuration using a delta connection (the most simple and basic configuration), the power flow in the multi-terminal DC system is easily controlled by the DC terminal voltage (see Figure 11).
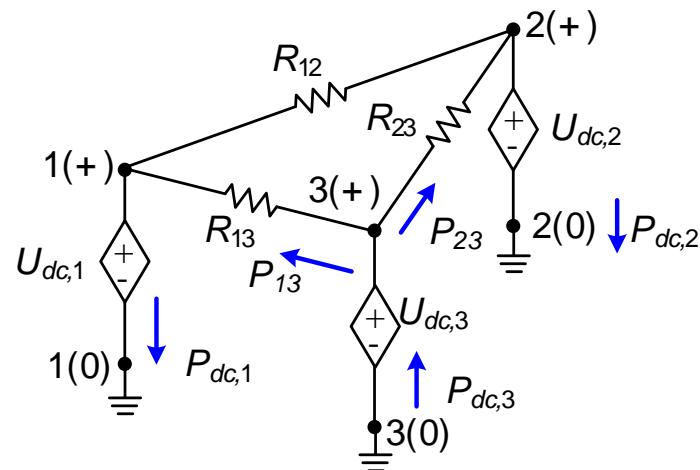
Figure 11. Circuital representation of monopole ideal ground return.

Cable 1–2 is basically an interconnector between the two onshore connection points, and it can be used to modulate the power injection/absorption at AC buses 4 and 5, where DC node 3 is the key component as WPP1 is injecting the power ($P_{dc,3} = P_{13} + P_{23}$). In this paper, the power flow of cable 1–3 and cable 2–3 are monitored.

Now, to illustrate the proposed coordinated controller, the active power injection/consumption of the two BESSs are used as the main control variable (P_{BESS1} and P_{BESS2}), and their SoCs are monitored (SoC_1 and SoC_2). The local state-of-charge controller is enabled to fulfill the following: $SoC_{min} = 10\% \leq SoC_k \leq SoC_{max} = 90\%$ ($k = 1, 2$). The DC power flows in cable 1–2, and cable 2–3 is taken as the decision variable. If $P_{12} > P^*_{12}$, BESS1 is charged (otherwise, discharged), and if $P_{23} > P^*_{23}$, BESS2 is charged (otherwise, discharged). The charging process of each distributed asset is controlled based on the SoC and active power injection/consumption. If $SoC_k \geq SoC_{max}$, stop charging. Charge if $SoC_{min} \leq SoC_k \leq SoC_{max}$, then the active power is discriminated between the nominal storing active power, power to start storing, and power to store at full power.

The multi-terminal MMC-HVDC stations are equipped with a local station controller, MMC-HVCD$_1$ and MMC-HVDC$_2$ are equipped with V_{dc}-Q_{ac} controller, where the reactive power production of the converter is adjusted to zero ($Q_{ac} = 0$); on the other hand, U_{dc1} and U_{dc2} are adjusted to 1.05 and 0.99 pu, respectively.

Initially, a quasi-dynamic simulation for a 24-h (1-min) resolution is performed to demonstrate the suitability of the proposed coordinated controller. The simulation results considering MMC-HVCD$_1$ and MMC-HVDC$_2$ equipped with V_{dc}-Q_{ac} controllers are shown in Figure 12. The proposed controller monitors the power flow at cable 1–3 (P_{13}) and cable 2–3 (P_{23}); when the power is above 15 MW, the correspondent BESS starts to charge ($SoC_0 = 50\%$), it is clear in Figure 11 that at 02:37 a.m., the power flows in those cables is reduced at BESS 2, stops charging for a period, and then continues; the SoC of both BESSs arrives to $SoC_{max} = 90\%$ is the power production in the offshore wind farm and the coordinated controller allows it, then the BESS reaches the maximum SoC and the centralised controller stops the power absorption. This preliminary simulation demonstrates the suitability of the proposed controller to fulfil a coordinated operation between the distributed BESS and offshore wind farm by the use of a multi-terminal MMC-HVDC systems.
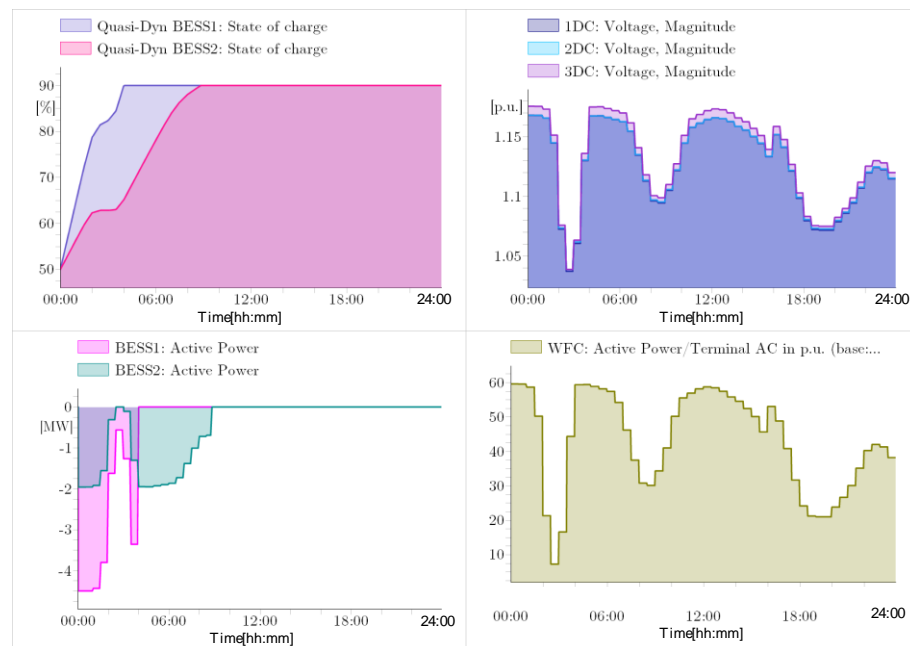
Figure 12. Simulation results: BESS1 and BESS2, $P_{dc,set1}$ = −5 MW, $P_{dc,set,2}$ = +5 MW, and ρ_{dc1} = ρ_{dc2} = 0.005 pu/MW. High wind speed.

Figures 13 and 14 show the performance of the proposed controller considering low wind speed and mid-wind speed, respectively; as the wind speed is reduced at the wind power plants, the active power production is reduced. However, the coordinated controller is able to charge the distributed BESS considering the control logic based on the cable DC power flow. As the wind speed is low, the power production is reduced, but the controller is able to charge the BESS. The time to reach the SOC_{max} = 90% is increased, but the controller is able to fulfil the objective.
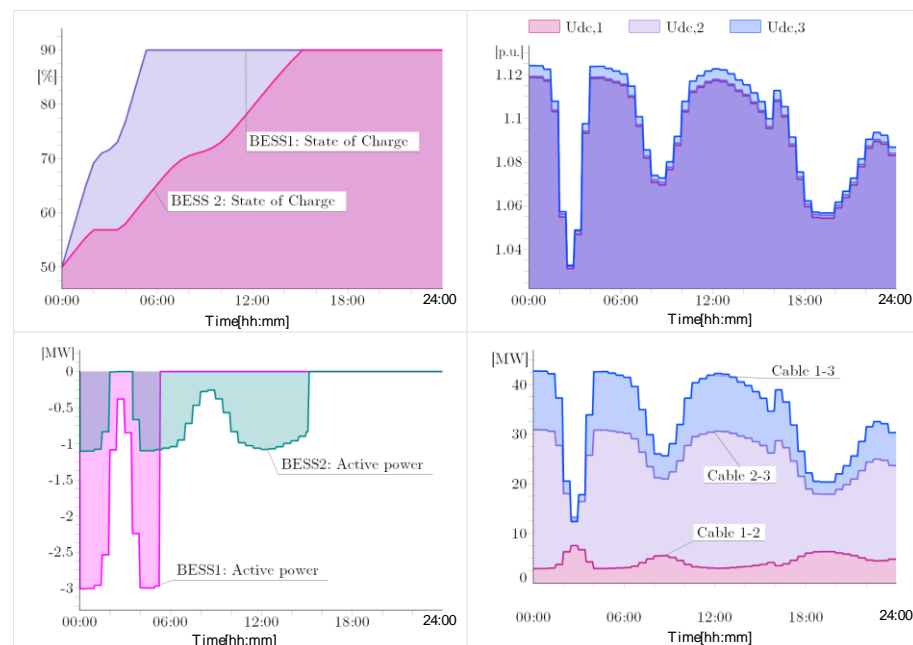

Figure 13. Simulation results: BESS1 and BESS2, $P_{dc,set1}$ = −5 MW, $P_{dc,set,2}$ = +5 MW, and ρ_{dc1} = ρ_{dc2} = 0.005 pu/MW. Average wind speed.

Figure 14. Simulation results: BESS1 and BESS2, $P_{dc,set1} = -5$ MW, $P_{dc,set,2} = +5$ MW, and $\rho_{dc1} = \rho_{dc2} = 0.005$ pu/MW. Low wind speed.

As the controller has been successfully tested and has demonstrated its suitability of the proposed approach, the final step is to assess the flexibility. The instantaneous active power flexibility of the whole AC−DC system is assessed. Figure 15 shows the balancing power required from the generator G1 without the proposed controller, and this time series is used as a base case to calculate the instantaneous flexibility power. The flexibility power, in this case, is obtained by the effective coordinated control of distributed-BESS and offshore wind farm via the multi-terminal MMC-HVDC system. Figures 16–18 show the time series plots of the balancing power required from the generator G1, considering three wind speed (high, mid, and low) scenarios at the offshore wind power plant and enabling the proposed controller.
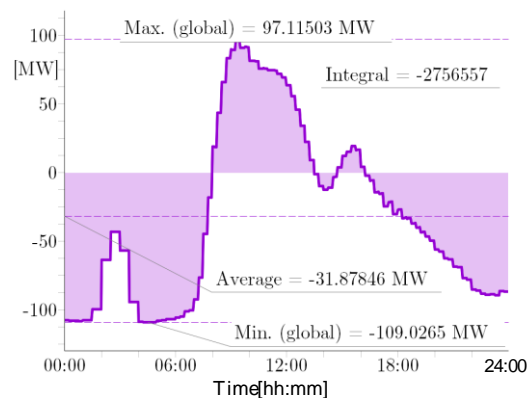

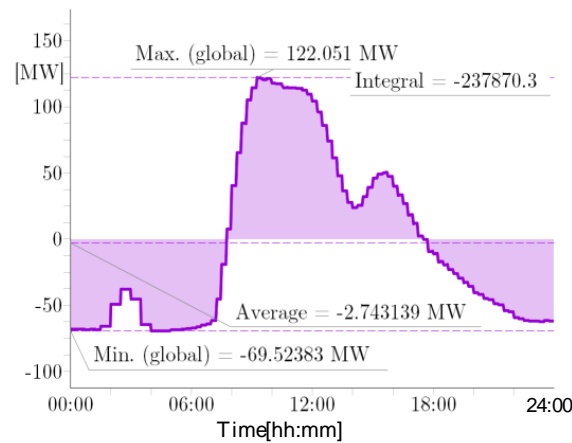**Figure 15.** Simulation results: balancing power, no coordinated control.

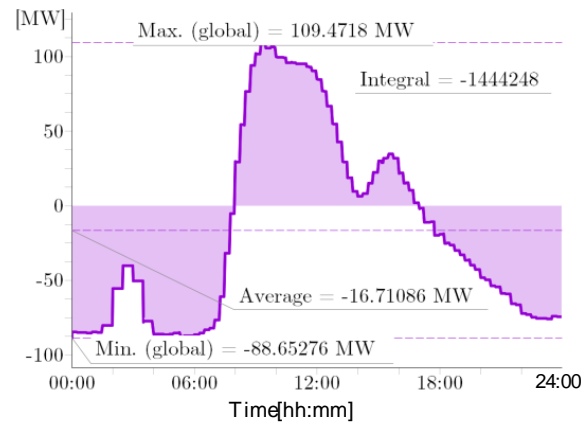**Figure 16.** Simulation results: balancing power, high-wind speed.

Figure 17. Simulation results: balancing power, mid-wind speed.
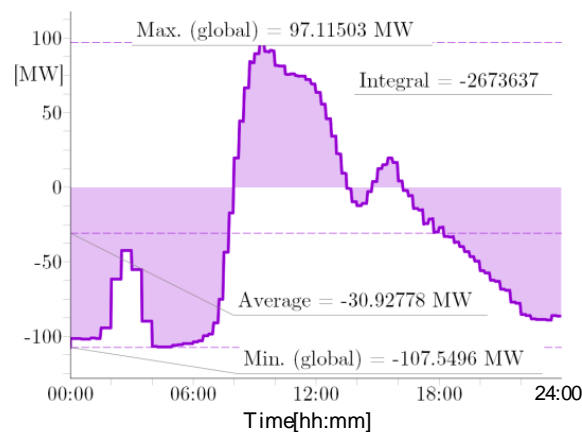

Figure 18. Simulation results: balancing power, low-wind speed.

Increasing the wind speed at the wind power plants increases the power generation, but the balancing power is also increased if the extra power is not appropriately diverted to the distributed-BESS by the proposed coordinated controller. However, the available instantaneous flexibility is strongly correlated with the changing pattern of the distributed assets (see Figure 19). It is, generally speaking, a property of the power system that describes its ability to cope with events that may cause imbalances between supply and demand at different time frames.
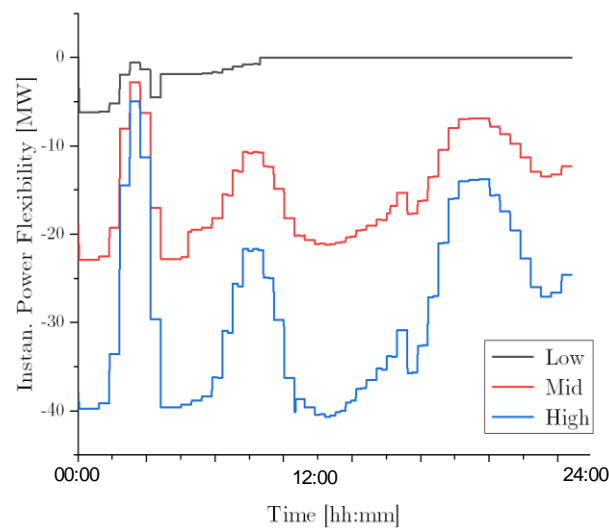
Figure 19. Simulation results: Instantaneous flexibility measured to the balancing power presented in Figure 15.

4. Conclusions

Modern power systems are facing several challenges; one of them is the massive penetration of variable renewable energy (VRE), especially for weather dependent technologies like wind and photovoltaic power. The growing volume of VRE increases the need to respond to the fluctuating needs of the power system, maintaining the security of the supply. The flexibility, generally speaking, refers to the property of the power system that describes its ability to cope with events that may cause imbalances between the supply and demand at different time frames. In this paper, a single layer coordinating controller is proposed and demonstrated. The single proposed layer coordinating controller is a closed-loop controller that uses wide-area measurements in the system to coordinate several transmission/distribution and energy storage assets. The controller uses a logic function to coordinate the steady-state operation of BESSs and wind power plants via a multi-terminal high voltage direct current (HVDC).

The single proposed layer coordinating controller is designed to build on the top of the local controller installed at the local assets, and uses low latency communication to implement the monitoring and control actions. One positive aspect of the proposed controller is that it has straightforward implementation. Digital communication is used for monitoring and control purposes; a centralised computer running the proposed algorithm is responsible for defining the control signals. As modern power converters are enabled to receive reference signals, the implementation of the proposed approach will not require drastic modifications at the BESSs, HVDC, or wind farm power converters. When compared with similar controllers, the proposed controller takes advantage of the local control functions enabled at the installed power converters; it reduces the computational burden of implementation. However, using the enabled control functions limits the flexibility of the approach, and exploring more complex and less traditional control strategies is not currently possible.

The proposed controller has been demonstrated using numerical simulations over a 24-h (1-min resolution) period using a customised version of the IEEE 14-bus test system, including a multi-terminal MMC-HVDC system. The controller has been implemented, and the capacity of fulfilling the defined control logic has been demonstrated. The instantaneous flexibility power has been used to assess the performance of the proposed controller. The results of the numerical simulations have demonstrated the suitability of the proposed coordinated controller to provide flexibility and decreasing requirements for balancing power.

References

1. International Renewable Energy Agency. *Power System Flexibility Metrics*; International Renewable Energy Agency: Abu Dhabi, United Arab Emirates, 2014; Volume 27.
2. CIGRE TB808 Working Group C5.27 Short-Term Flexibility in Power Systems: Drivers and Solutions. Available online: https://electra.cigre.org/311-august-2020/technical-brochures/short-term-flexibility-in-power-systems-drivers-and-solutions.html. (accessed on 1 May 2021).
3. Energy UK Defining Flexibility 2018. Available online: https://www.energy-uk.org.uk/publication.html?task=file.download&id=6625#:~{}:text=Flexibility (accessed on 8 May 2021).
4. Nosair, H.; Bouffard, F. Flexibility Envelopes for Power System Operational Planning. *IEEE Trans. Sustain. Energy* **2015**, *6*, 800–809. [CrossRef]
5. Zhao, J.; Zheng, T.; Litvinov, E. A Unified Framework for Defining and Measuring Flexibility in Power System. *IEEE Trans. Power Syst.* **2016**, *31*, 339–347. [CrossRef]
6. Bucher, M.A.; Chatzivasileiadis, S.; Andersson, G. Managing Flexibility in Multi-Area Power Systems. *IEEE Trans. Power Syst.* **2016**, *31*, 1218–1226. [CrossRef]
7. Lannoye, E.; Flynn, D.; O'Malley, M. Evaluation of Power System Flexibility. *IEEE Trans. Power Syst.* **2012**, *27*, 922–931. [CrossRef]
8. Thatte, A.A.; Xie, L. A Metric and Market Construct of Inter-Temporal Flexibility in Time-Coupled Economic Dispatch. *IEEE Trans. Power Syst.* **2016**, *31*, 3437–3446. [CrossRef]
9. Hargreaves, J.; Hart, E.K.; Jones, R.; Olson, A. Reflex: An Adapted Production Simulation Methodology for Flexible Capacity Planning. *IEEE Trans. Power Syst.* **2015**, *30*, 1306–1315. [CrossRef]
10. Yasuda, Y.; Årdal, A.R.; Huertas-Hernando, D.; Carlini, E.M.; Estanqueiro, A.; Flynn, D.; Gomez-Lazaro, E.; Holttinen, H.; Kiviluoma, J.; van Hulle, F.; et al. Flexibility Chart: Evaluation on diversity of flexibility in various areas. In Proceedings of the 12th International Workshop on Large-Scale Integration of Wind Power into Power Systems as well as on Transmission Networks for Offshore Wind Farms, WIW2013, London, UK, 22–24 October 2013.
11. Wang, Y.; Zhao, S.; Zhou, Z.; Botterud, A.; Xu, Y.; Chen, R. Risk Adjustable Day-Ahead Unit Commitment With Wind Power Based on Chance Constrained Goal Programming. *IEEE Trans. Sustain. Energy* **2017**, *8*, 530–541. [CrossRef]
12. Ye, H.; Wang, J.; Ge, Y.; Li, J.; Li, Z. Robust Integration of High-Level Dispatchable Renewables in Power System Operation. *IEEE Trans. Sustain. Energy* **2017**, *8*, 826–835. [CrossRef]
13. Shao, C.; Wang, X.; Shahidehpour, M.; Wang, X.; Wang, B. Security-Constrained Unit Commitment With Flexible Uncertainty Set for Variable Wind Power. *IEEE Trans. Sustain. Energy* **2017**, *8*, 1237–1246. [CrossRef]
14. Khan, S.; Gawlik, W.; Palensky, P. Reserve Capability Assessment Considering Correlated Uncertainty in Microgrid. *IEEE Trans. Sustain. Energy* **2016**, *7*, 637–646. [CrossRef]
15. Li, W.; Tesfatsion, L. Market provision of flexible energy/reserve contracts: Optimisation formulation. In Proceedings of the 2016 IEEE Power and Energy Society General Meeting (PESGM), Boston, MA, USA, 17–21 July 2016; pp. 1–5.
16. Cornelius, A.; Bandyopadhyay, R.; Patiño-Echeverri, D. Assessing environmental, economic, and reliability impacts of flexible ramp products in MISO's electricity market. *Renew. Sustain. Energy Rev.* **2018**, *81*, 2291–2298. [CrossRef]
17. Marneris, I.G.; Biskas, P.N.; Bakirtzis, E.A. An Integrated Scheduling Approach to Underpin Flexibility in European Power Systems. *IEEE Trans. Sustain. Energy* **2016**, *7*, 647–657. [CrossRef]
18. Wang, B.; Hobbs, B.F. Real-Time Markets for Flexiramp: A Stochastic Unit Commitment-Based Analysis. *IEEE Trans. Power Syst.* **2016**, *31*, 846–860. [CrossRef]
19. Després, J.; Mima, S.; Kitous, A.; Criqui, P.; Hadjsaid, N.; Noirot, I. Storage as a flexibility option in power systems with high shares of variable renewable energy sources: A Poles-based analysis. *Energy Econ.* **2017**, *64*, 638–650. [CrossRef]
20. Koltsaklis, N.E.; Dagoumas, A.S.; Georgiadis, M.C.; Papaioannou, G.; Dikaiakos, C. A mid-term, market-based power systems planning model. *Appl. Energy* **2016**, *179*, 17–35. [CrossRef]
21. Koltsaklis, N.E.; Dagoumas, A.S.; Panapakidis, I.P. Impact of the penetration of renewables on flexibility needs. *Energy Policy* **2017**, *109*, 360–369. [CrossRef]

22. Milligan, M.; Frew, B.A.; Bloom, A.; Ela, E.; Botterud, A.; Townsend, A.; Levin, T. Wholesale electricity market design with increasing levels of renewable generation: Revenue sufficiency and long-term reliability. *Electr. J.* **2016**, *29*, 26–38. [CrossRef]

23. Mancini, F.; Cimaglia, J.; Lo Basso, G.; Romano, S. Implementation and Simulation of Real Load Shifting Scenarios Based on a Flexibility Price Market Strategy—The Italian Residential Sector as a Case Study. *Energies* **2021**, *14*, 3080. [CrossRef]

24. Mendicino, L.; Menniti, D.; Pinnarelli, A.; Sorrentino, N.; Vizza, P.; Alberti, C.; Dura, F. DSO Flexibility Market Framework for Renewable Energy Community of Nanogrids. *Energies* **2021**, *14*, 3460. [CrossRef]

25. Eid, C.; Codani, P.; Perez, Y.; Reneses, J.; Hakvoort, R. Managing electric flexibility from Distributed Energy Resources: A review of incentives for market design. *Renew. Sustain. Energy Rev.* **2016**, *64*, 237–247. [CrossRef]

26. Brijs, T.; De Jonghe, C.; Hobbs, B.F.; Belmans, R. Interactions between the design of short-term electricity markets in the CWE region and power system flexibility. *Appl. Energy* **2017**, *195*, 36–51. [CrossRef]

27. Akrami, A.; Doostizadeh, M.; Aminifar, F. Power system flexibility: An overview of emergence to evolution. *J. Mod. Power Syst. Clean Energy* **2019**, *7*, 987–1007. [CrossRef]

28. Miranda, T.; Delgado-Gomes, V.; Martins, J.F. On the use of IEC 61850-90-7 for Smart Inverters Integration. In Proceedings of the 2018 International Conference on Intelligent Systems (IS), Madeira, Portuga, 25–27 September 2018; pp. 722–726.

29. Van Hertem, D.; Oriol Gomiz-Bellmunt, J.L. *HVDC GRIDS: For Offshore and Supergrid of the Future*; JohnWiley & Sons, Inc.: Hoboken, NJ, USA, 2016; ISBN 9789004310087.

30. Springer. *Modelling and Simulation of Power Electronic Converter Dominated Power Systems in PowerFactory*; Gonzalez-Longatt, F.M., Rueda Torres, J.L., Eds.; Springer International Publishing: Cham, Switzerland, 2021; ISBN 978-3-030-54123-1.

31. Gonzalez-Longatt, F.; Roldan, J. Effects of DC Voltage control strategy on voltage response on multi-terminal HVDC following loss of a converter station. In Proceedings of the IEEE Power and Energy Society General Meeting, Vancouver, BC, Canada, 21–25 July 2013.

32. Gonzalez-Longatt, F.; Roldan, J.M. Effects of dc voltage control strategies of voltage response on multi-terminal HVDC following a disturbance. In Proceedings of the 47th International Universities Power Engineering Conference (UPEC), Middlesex, UK, 4–7 September 2012; pp. 1–6.

33. Chamorro, H.R.; Torkzadeh, R.; Kotb, O.; Rouzbehi, K.; Escaño, J.M.; Gonzalez-Longatt, F.; Bellmunt, O.G.; Toma, L.; Sood, V.K. On the Optimisation of Damping Enhancement in a Power System with a Hybrid HVDC Link. In Proceedings of the 2019 IEEE PES Innovative Smart Grid Technologies Europe, ISGT-Europe 2019, Bucharest, Romania, 29 September–2 October 2019.

34. Gonzalez-Longatt, F.M.; Roldan, J.M.; Rueda, J.L. Impact of DC control strategies on dynamic behaviour of multi-terminal voltage-source converter-based HVDC after sudden disconnection of a converter station. In Proceedings of the 2013 IEEE Grenoble Conference PowerTech, POWERTECH 2013, Grenoble, France, 16–20 June 2013.

35. Gonzalez-Longatt, F.M. Effects of Fast Acting Power Controller of BESS in the System Frequency Response of a Multi-Machine System: Probabilistic Approach. In Proceedings of the 2018 IEEE Innovative Smart Grid Technologies—Asia (ISGT Asia), Singapore, 22–25 May 2018; pp. 798–803.

36. Acosta, M.N.; Pettersen, D.; Gonzalez-Longatt, F.; Peredo Argos, J.; Andrade, M.A. Optimal Frequency Support of Variable-Speed Hydropower Plants at Telemark and Vestfold, Norway: Future Scenarios of Nordic Power System. *Energies* **2020**, *13*, 3377. [CrossRef]

37. Gonzalez-Longatt, F.; Alhejaj, S.; Marano-Marcolini, A.; Rueda Torres, J.L. Probabilistic Load-Flow Using Analysis Using DPL Scripting Language. In *Green Energy and Technology*; Springer: Berlin/Heidelberg, Germany, 2018; pp. 93–124.